

Dithienophosphole-capped π -conjugated oligomers†‡§

Stefan Durben, Thomas Linder and Thomas Baumgartner*

Received (in Montpellier, France) 15th January 2010, Accepted 2nd March 2010

DOI: 10.1039/c0nj00026d

The synthesis of a 2-monobrominated dithieno[3,2-*b*:2',3'-*d*]phosphole has opened the access to a series of highly luminescent π -conjugated oligomers that link two dithienophosphole units *via* a variety of aromatic spacers. The nature of the linking mode was found to have a significant impact on the photophysical properties of the system as a whole, either considerably improving the molar absorptivity of the new extended chromophores, or providing luminescent materials with red-shifted emission features and substantial photoluminescence quantum yields.

Introduction

The intriguing optical and electronic properties of organic π -conjugated materials have led to the significant growth and considerable importance of organic electronics in recent years. The intrinsic semiconducting properties of these materials make them excellent candidates for a variety of optoelectronic applications, such as Organic Light-Emitting Diodes (OLEDs), Organic Photovoltaic Cells (OPVs), and Organic Field-Effect Transistors (OFETs), among others.¹ The inherent benefits of using organic components include an almost infinite pool of synthons that can be incorporated in these materials, allowing for the possibility of tailoring the materials properties towards specific applications. Although purely organic components have proven to be quite a useful resource for the synthesis of organic electronic materials, inorganic main group components have recently started to draw an increasing amount of attention in this context. Particularly, organoboron-,² organosilicon-,³ and organophosphorus-based⁴ π -conjugated materials have proven to be very valuable for this purpose. Due to their unique nature, in terms of electronics and chemistry, inorganic components provide unprecedented (with purely organic based materials) opportunities to significantly tune the materials' electronics. Whereas boron provides an empty p-orbital that can effectively overlap with a π -conjugated scaffold, silicon and phosphorus have shown a peculiar interaction involving the π -conjugated scaffold—the π^* -orbital in particular—and the antibonding σ^* -orbitals of exocyclic Si/P–C bonds that both lower the LUMO levels of the materials significantly.^{2–4} These electronic effects are much more pronounced than those of purely organic units and illustrate the highly valuable nature of the main group approach toward organic electronics.

In this context we have established the dithieno[3,2-*b*:2',3'-*d*]phosphole system over the past seven years or so and were able

to systematically address a variety of important features targeted toward certain applications.⁵ Our studies have shown that dithienophosphole is an exceptionally strong chromophore with impressive quantum yields ranging from 50–90%. We were further able to fine tune the properties of molecular building blocks (*i.e.*, emission colors and semiconducting behavior),⁶ as well as to access polymeric materials with desirable photophysical properties and processability features.⁷

In this contribution we now report the synthesis and advanced characterization of a series of π -conjugated oligomers that showcase two dithienophosphole units as 'end-caps' linked by different aromatic spacers. We were interested, if the unprecedented photophysical properties of dithienophosphole-based materials can be enhanced through the presence of two units within the same material. Furthermore, we wanted to investigate how the linking mode of the two dithienophosphole units affects the photophysical properties of the materials as a whole.

Results and discussion

Synthesis and characterization of 2-bromodithieno[3,2-*b*:2',3'-*d*]phosphole oxide

To be able to install the dithienophosphole moiety as an end cap, mono-functionalization of the scaffold was deemed necessary. Recently, a 2-iododithieno[3,2-*b*:2',3'-*d*]phosphole oxide has been reported by our group as precursor for highly luminescent dithienophosphole-containing terpyridinyl complexes,⁸ representing the first example of monofunctionalized dithienophosphole building blocks. Starting point for the work presented here is the corresponding bromo-derivative **2** (BrS₂PO), which was prepared by rapid addition of one equivalent *N*-bromosuccinimide (NBS) to dithienophosphole oxide **1** (S₂PO) in dimethylformamide solution at 0 °C (Scheme 1). Under these conditions, the reaction proceeds extremely fast, meaning that the conversion is complete immediately after addition of the brominating reagent. Unfortunately, dibromination in the 2- and 6-positions^{6b} seems to be favored over the desired monobromination. In an attempt to optimize the reaction it was found that traces of 2,6-dibrominated product **3** (Br₂S₂PO) started to form upon

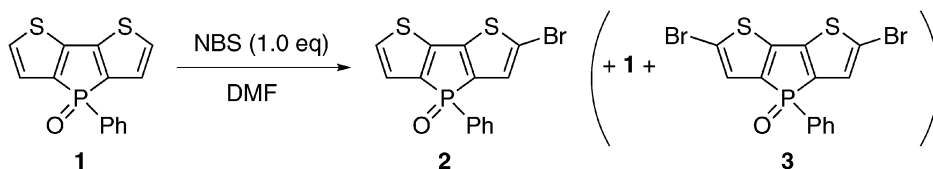
Department of Chemistry, University of Calgary, 2500 University Dr. NW, Calgary AB, T2N 1N4, Canada.

E-mail: thomas.baumgartner@ucalgary.ca; Fax: +1 403-289-9488

† This article is part of a themed issue on Main Group chemistry.

‡ In memory of Pascal Le Floch, an esteemed member of the phosphorus family.

§ CCDC reference number 761478 (2). For crystallographic data in CIF format see DOI: 10.1039/c0nj00026d



Scheme 1 Synthesis of monobrominated dithienophosphole **2**.

addition of only 0.3 equivalents of NBS, indicating that the reactivity of 2-bromodithienophosphole oxide **2** towards NBS is significantly higher than that of non-halogenated oxide **1**.

The previously reported 2-iododithieno[3,2-*b*:2',3'-*d'*]phosphole could be conveniently separated from the product mixture with cold dichloromethane.⁸ Similar procedures with a variety of solvents were attempted for the purification of **2**, however, due to the similar solubility of mono- and dibrominated species **2** and **3**, none of these methods were successful. For the same reason, crystallization from a variety of different solvent mixtures did not provide pure product. Column chromatography on silica gel with chloroform/ethyl acetate (1/1) was established to be the most successful method for the separation of non-, mono- and dibrominated product. Due to the polar nature of phosphole oxides, retention factors for **1–3** are low ($R_f = 0.4–0.5$). Even though tedious, the effort leads to pure compound **2** in moderate yields (61%). Typically, ~10% of starting material **1** and ~15% of dibromide **3** are also recovered. The formation of **2** is supported by a significant change in the ^1H NMR spectrum, clearly showing the presence of an asymmetric species. To a lesser extent, the ^{31}P NMR resonance also supports the monobrominated product with a chemical shift of $\delta^{31}\text{P}$ 18.9 ppm, which lies in between the resonance frequencies for **1** ($\delta^{31}\text{P}$ 18.7 ppm) and **3** ($\delta^{31}\text{P}$ 19.1 ppm).

Single crystals of **2**, suitable for X-ray crystallography, could be obtained from a concentrated acetone solution (Table 1). The solid state structure (Fig. 1, top) of the monobrominated dithienophosphole exhibits a planar dithienophosphole scaffold, indicating a high degree of π -conjugation. As a result of the monofunctionalization, the pyramidal phosphorus atom becomes a stereocenter. Both enantiomers are present in the unit

cell. All bond lengths of the dithienophosphole scaffold are in very good agreement to previously reported dithienophosphole oxides.^{5b,6b} The monobromination seems to have only minor influence on the annelated framework. In the crystal packing (Fig. 1, bottom), however, the presence of the bromine results in short intermolecular bromine–oxygen contacts of 2.97 Å that had been observed in the packing of a dibrominated dithienophosphole before.⁹ In addition, the crystal structure exhibits coplanar face-to-face interactions between the dithienophosphole backbone of neighboring molecules (3.75 Å), and the phenyl substituents of neighboring molecules (3.60 Å), respectively.

The photophysical properties of the new monobrominated dithienophosphole were determined in dilute methylene chloride solution ($c = 10^{-5}$ M) and show, in comparison to

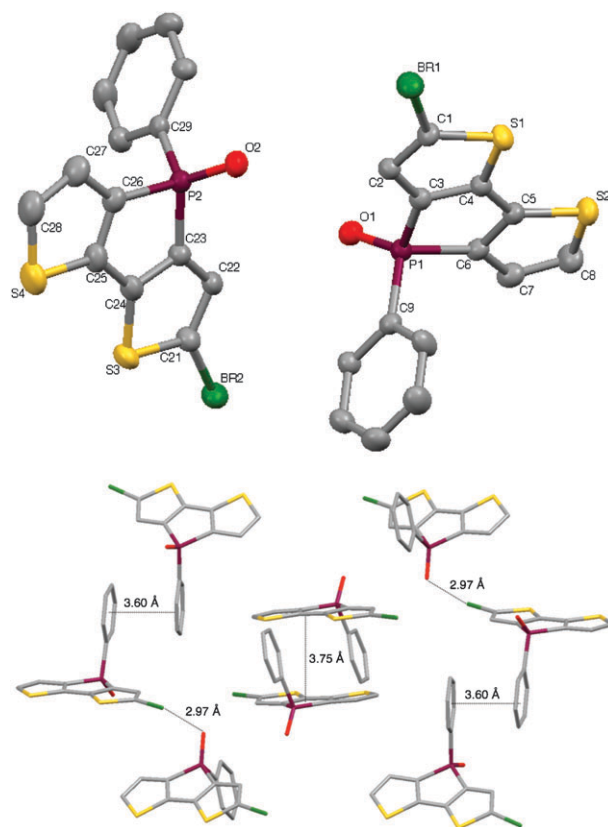


Fig. 1 Molecular structure of **2** (top) and packing (bottom) in the solid state (50% probability level, hydrogens are omitted for clarity). Selected bond lengths [Å]: P1–C3 1.805(5), P1–C6 1.814(5), P1–C9 1.806(5), BR1–C1 1.859(5), C1–C2 1.362(6), C2–C3 1.419(6), C3–C4 1.369(6), C4–C5 1.454(6), C5–C6 1.389(7), C6–C7 1.409(7), C7–C8 1.367(8), P2–C23 1.807(5), P2–C26 1.812(5), P2–C29 1.789(5), BR2–C21 1.858(5), C21–C22 1.376(7), C22–C23 1.410(7), C23–C24 1.379(6), C24–C25 1.445(7), C25–C26 1.380(7), C26–C27 1.423(7), C27–C28 1.356(8).

Table 1 Crystal data and data collection details for **2**

Empirical formula	C ₁₄ H ₈ BrOPS ₂
Formula weight	734.41
Crystal system	Monoclinic
Space group	<i>P</i> 2 ₁ / <i>c</i>
<i>a</i> /Å	19.5034(6)
<i>b</i> /Å	8.3637(2)
<i>c</i> /Å	18.1644(6)
β /°	105.2595(11)
<i>V</i> /Å ³	2858.52(15)
<i>Z</i>	4
<i>D</i> _{calc} /g cm ^{−3}	1.706
<i>T</i> /K	293
<i>F</i> (000)	1456
μ /mm ^{−1}	3.267
Reflections collected	10 482
Unique reflections	6410
Observed reflections	5391
<i>R</i> indices (all data)	<i>R</i> _{int} = 0.0292 <i>R</i> ₁ = 0.0698 <i>wR</i> ₂ = 0.1743

Table 2 Photophysical data and calculated frontier orbital energies for **1–5**

Compound	$\lambda_{\text{abs}}^a/\text{nm}$	$\epsilon_{\text{max}}^a/\text{L mol}^{-1} \text{ cm}^{-1}$	$\lambda_{\text{ex}}^b/\text{nm}$	$\lambda_{\text{em}}^b/\text{nm}$	ϕ_{PL}^c	$E_{\text{HOMO}}^d/\text{eV}$	$E_{\text{LUMO}}^d/\text{eV}$	$\Delta E_{\text{bg}}^d/\text{eV}$
1	362	6650	365	453	0.57	—	—	—
2	374	7800	382	465	0.54	—	—	—
3 ^{6b}	384	9450	397	473	0.57	—	—	—
4a	428	19 550	432	498	0.32	−5.32	−2.28	3.04
4b	397	25 650	402	481	0.47	−5.28	−2.72/−2.64	2.56/2.64
4c	416	75 800	421	489	0.21	−5.34	−2.19	3.15
4d	430	38 400	437	500	0.19	−5.23	−2.18	3.05
5	465	41 900	458	544	0.80	−5.06	−2.42	2.64

^a UV/VIS absorption in CH_2Cl_2 . ^b Fluorescence excitation and emission maxima in CH_2Cl_2 . ^c Photoluminescence quantum yields in CH_2Cl_2 solution, relative to quinine sulfate (**1–4**) or fluorescein (**5**). ^d Calculated energies, B3LYP/6-31G*.

1, red-shifted excitation and emission features due to a decrease of the LUMO energy as a result of the electron withdrawing nature of the halogen atom (Table 2).^{6b} The excitation and emission wavelengths of **2** ($\lambda_{\text{ex}} = 382 \text{ nm}$, $\lambda_{\text{em}} = 465 \text{ nm}$) are red-shifted from the starting material **1** ($\lambda_{\text{ex}} = 365 \text{ nm}$, $\lambda_{\text{em}} = 453 \text{ nm}$) by 17 nm and 12 nm, respectively. Upon introduction of a second bromine in the 6-position (**3**, $\lambda_{\text{ex}} = 397 \text{ nm}$, $\lambda_{\text{em}} = 473 \text{ nm}$),^{6b} the excitation and emission bands experience a further bathochromic shift by 15 nm and 8 nm, respectively, which represents an almost linear dependence of the photophysical features on the degree of bromination. Monobrominated compound **2** shows a high photoluminescence quantum yield ($\phi_{\text{PL}} = 54\%$), comparable to those previously reported for **1** ($\phi_{\text{PL}} = 57\%$) and **3** ($\phi_{\text{PL}} = 57\%$). The UV/VIS absorption spectra (Fig. 2) follow the same quasi-linear trend for the absorption wavelengths of the π - π^* -transition with increasing degree of bromination (**1**: $\lambda_{\text{abs}} = 362 \text{ nm}$; **2**: $\lambda_{\text{abs}} = 374 \text{ nm}$; **3**: $\lambda_{\text{abs}} = 384 \text{ nm}$).

An increase of the absorption coefficient was observed with increasing number of bromine atoms present (**1**: $\epsilon(362) = 6650 \text{ L mol}^{-1} \text{ cm}^{-1}$; **2**: $\epsilon(374) = 7800 \text{ L mol}^{-1} \text{ cm}^{-1}$; **3**: $\epsilon(384) = 9450 \text{ L mol}^{-1} \text{ cm}^{-1}$). Participation of bromine lone pairs in the π -conjugation, or an increased cross-section could explain this behavior.

Synthesis and characterization of cross-coupled oligomers

The monobrominated dithienophosphole oxide **2** was subsequently used as starting material for the synthesis of a series of π -conjugated oligomers *via* an established Suzuki–Miyaura cross-coupling protocol (Scheme 2). In previous studies,^{5b,6b,7b,8} the oxidized phosphorus center proved to be very tolerant to subsequent cross-coupling reactions, as it prevents coordination of the phosphorus to palladium, which is commonly used as catalyst for a variety of carbon–carbon bond forming reactions, such as Heck–Cassar–Sonogashira-, Suzuki–Miyaura- or Stille-reactions.¹⁰ In order to investigate the effects of different conjugation-pathways and -lengths, a series of oligomers with benzene-derived linkers **4a–d** was targeted. In addition, the effect of a heteroarene-bridge was examined in compound **5**. Suzuki–Miyaura coupling of **2** with the corresponding diboronic acids in a biphasic (toluene/water) mixture^{6b,10} afforded the short chains **4a–d** as yellow to orange solids in moderate yields. The bithiophene-bridged compound **5** was obtained as dark orange solid in moderate yield from the reaction of **2** with 2,2'-bithiophene-5,5'-diboronic acid bis(pinacole) ester¹¹ in tetrahydrofuran solution. All coupled

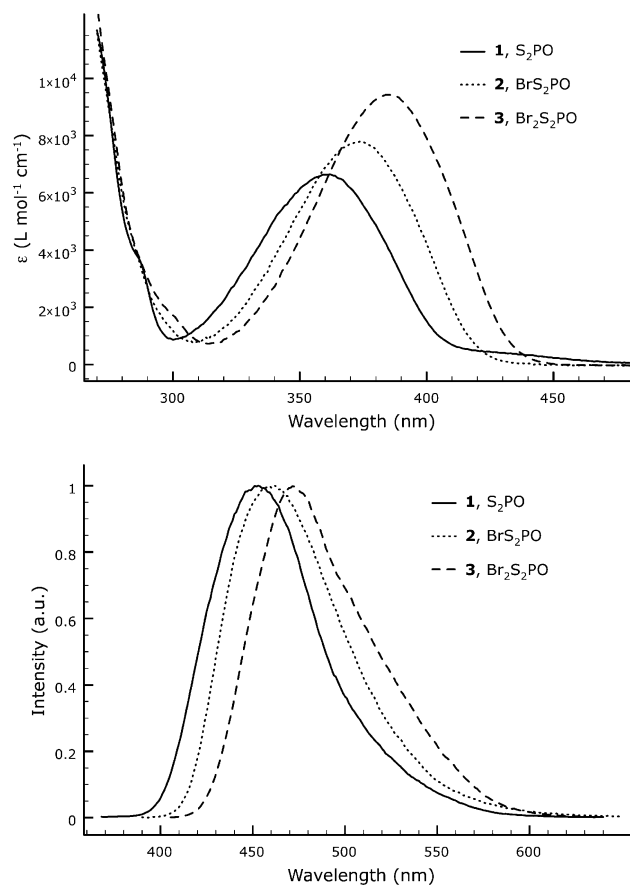
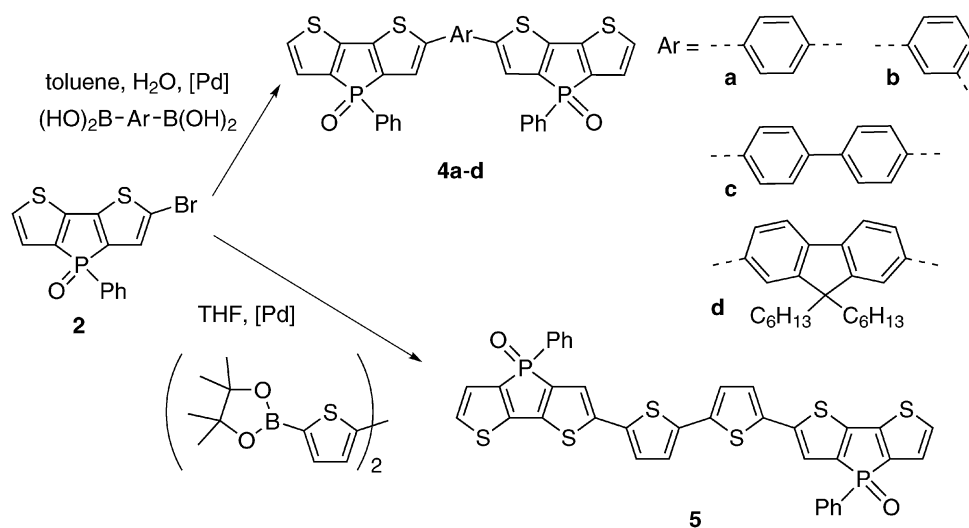


Fig. 2 UV/VIS absorption (top) and normalized emission spectra (bottom) of **1–3** in CH_2Cl_2 solution.

compounds show slightly downfield shifted ^{31}P NMR resonances ($\delta^{31}\text{P}$ 19.2–19.6 ppm) compared to that of **2** ($\delta^{31}\text{P}$ 18.9). In the case of the hydrocarbon linked systems **4a–d**, the highly diagnostic ^1H NMR signal for the proton in the 3-position of the dithienophosphole scaffold experiences a characteristic downfield shift ($\delta^1\text{H}$ 7.37–7.42 ppm) when compared to the corresponding signal in the starting material **2** ($\delta^1\text{H}$ 7.12 ppm). This effect is far less pronounced in the bithiophene-linked oligomer **5** ($\delta^1\text{H}$ 7.19 ppm), potentially due to some sulfur–hydrogen interactions.

All cross-coupled oligomers feature two phosphorus stereocenters, giving rise to three possible diastereomers in statistical distribution. Even though all diastereomers must be



Scheme 2 Synthesis of dithienophosphole-capped oligomers.

present, it was impossible to separately characterize them, since only a single set of NMR-signals was observed in each case. The 1,3- and 1,4-benzene bridged compounds **4a,b** were purified by column chromatography, but no separation of the diastereomers was observed. The separation of the diastereomers would have been desirable in order to increase the chance of crystallizing the oligomers but none of the materials formed single crystals suitable for X-ray crystallography. The latter, on the other hand, is a beneficial feature, as crystallinity and resulting solid-state quenching effects often reduce the applicability of these compounds in optoelectronic devices.¹

Upon extension of the π -conjugated system, all photophysical features are significantly red-shifted from those of starting material **2** (Table 2). The smallest bathochromic shift is observed with the 1,3-benzene-bridged oligomer **4b** ($\lambda_{\text{ex}} = 402$ nm, $\lambda_{\text{em}} = 481$ nm), due to the somewhat disrupted conjugation path through the 1,3-benzene link. Surprisingly, the 4,4'-biphenyl-linked chain **4c** shows only slightly red-shifted excitation and emission features ($\lambda_{\text{ex}} = 421$ nm, $\lambda_{\text{em}} = 489$ nm) compared to **4b**. This is probably due to the non-coplanar structure of biphenyl, leading to a disrupted conjugation path and electronic decoupling into two separate fluorophores. The 1,4-benzene- and the 2,7-fluorene-bridged compounds **4a** and **4d** show almost identical maxima of excitation and emission (**4a**: $\lambda_{\text{ex}} = 432$ nm, $\lambda_{\text{em}} = 498$ nm; **4d**: $\lambda_{\text{ex}} = 437$ nm, $\lambda_{\text{em}} = 500$ nm), giving rise to the assumption that a comparable effective conjugation length is present in both molecules. In the case of the bithiophene-bridged molecule **5**, excitation and emission features are most significantly red-shifted ($\lambda_{\text{ex}} = 458$ nm, $\lambda_{\text{em}} = 544$ nm), probably due to a more planar structure and electron donating nature of the electron-rich linker (Fig. 3).

UV/VIS absorption maxima are in very good agreement with the excitation data. The extinction coefficients rise in the order **4a** < **4b** < **4d** < **5** < **4c** (Table 2). The fact that **4b** has a higher absorption coefficient than **4a** was surprising, however, theoretical calculations showed a two-fold degenerate LUMO in **4b** (Fig. 4) that very likely leads to a significant increase ($\Delta\epsilon$ 6100 L mol⁻¹ cm⁻¹) of the absorption coefficient.

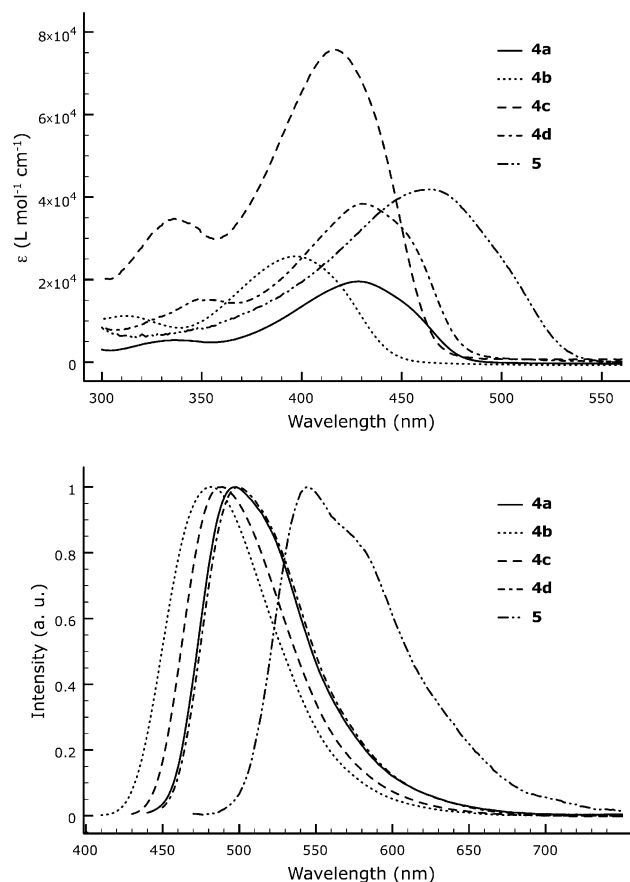


Fig. 3 UV/VIS absorption (top) and normalized emission spectra (bottom) of **4a-d** and **5** in CH₂Cl₂ solution.

Compounds **4d** and **5** showed significantly increased molar absorptivities (**4d**: $\epsilon(430) = 38\,400$ L mol⁻¹ cm⁻¹; **5**: $\epsilon(465) = 41\,900$ L mol⁻¹ cm⁻¹) compared to **4a** and **b** due to their extended π -conjugated system and high planarity. The highest absorptivity was observed in compound **4c** ($\epsilon(416) = 75\,800$ L mol⁻¹ cm⁻¹), which can be explained by the non-coplanar nature of the biphenyl linker, resulting in the

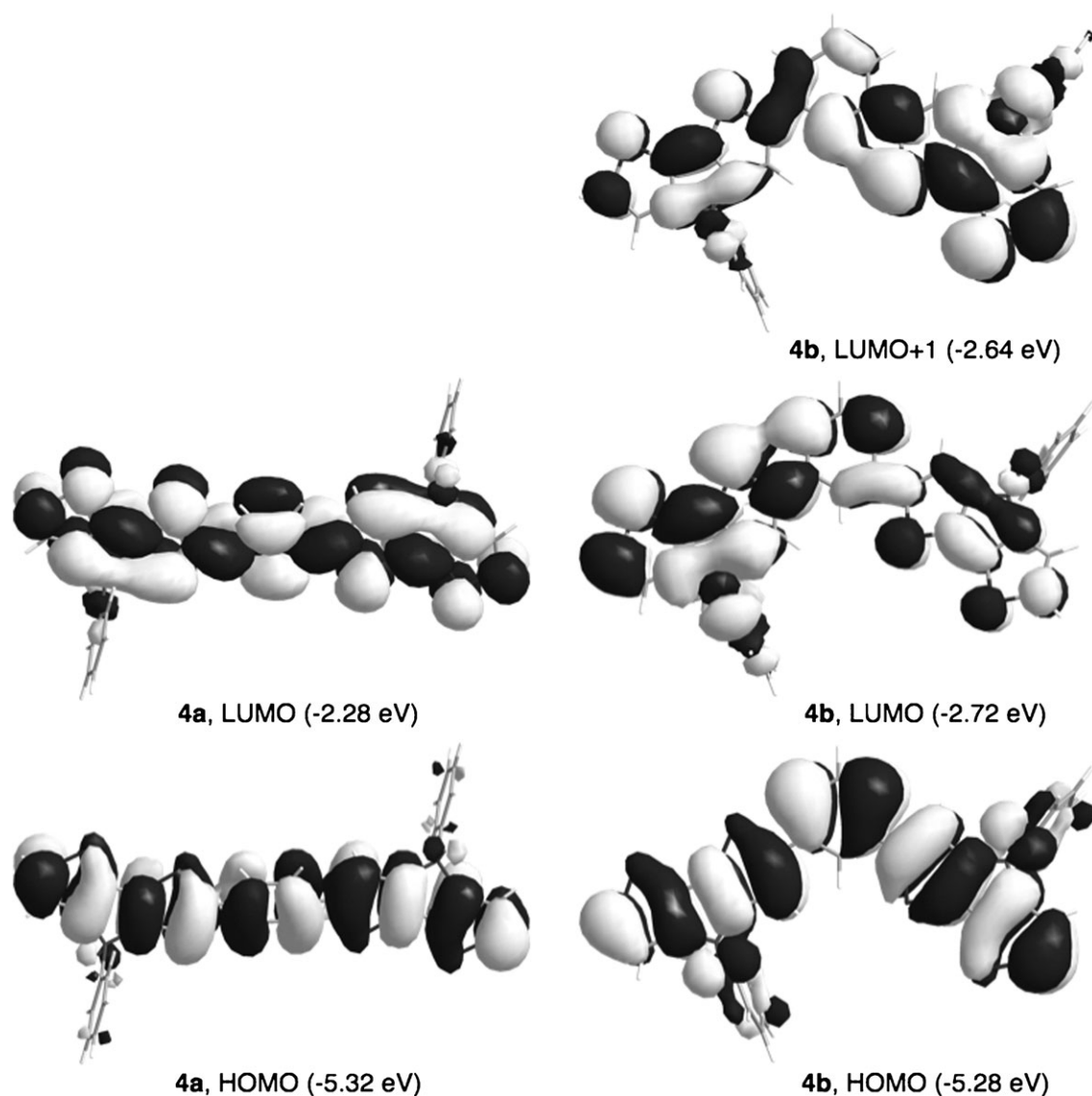


Fig. 4 Frontier orbital diagrams of **4a** (left) and **4b** (right).

formation of two separate chromophores in one molecule. The photoluminescence quantum yields for the hydrocarbon-linked compounds **4a–d** are moderate to good (Table 2), probably due to some degree of rotational freedom between the dithienophosphole end groups and the linker. The bithiophene-bridged oligomer **5** shows a very high photoluminescence quantum efficiency ($\phi_{\text{PL}} = 80\%$), which is very likely caused by the fixated coplanar structure of the thiophene units.

In order to gain a deeper understanding of the electronic structure of the oligomers, DFT calculations at the B3LYP/6-31G* level of theory were performed.¹² All oligomers show coplanar or only slightly twisted structures with, **4b** excepted, frontier orbitals extending over the entire conjugated backbone. The frontier orbitals of compound **4a** are shown as an example (Fig. 4). As mentioned above, the 1,3-benzene linked derivative **4b** shows a two-fold degeneration ($\Delta E < 0.1$ eV) of the LUMO orbital (Fig. 4), resulting in an increased molar absorptivity compared to **4a**, despite a disrupted conjugation

path in the spacer. In accordance with previous studies,^{4c–f,5,6c,8} the phosphorus centers exclusively contribute to the LUMO, offering the unique possibility of tuning the LUMO energies by functionalization of the phosphorus centers. Compounds **4a–d** show consistently low-lying HOMO energies ($E_{\text{HOMO}} = -5.34$ to -5.23 eV), illustrating the stabilizing effect of moderately electron-poor spacers. In contrast to that, a destabilized HOMO-level ($E_{\text{HOMO}} = -5.06$ eV) is observed in **5**, due to the electron-rich linker. The LUMO energies of **4a,c,d** are also similar ($E_{\text{LUMO}} = -2.28$ to -2.18 eV). Compound **4b**, however, shows a significantly stabilized LUMO energy as an effect of the degeneration. The bithiophene-bridged oligomer **5** shows a low-lying LUMO compared to **4a,c,d** due to the presence of electron-deficient end-groups attached to a linker with high electron-density, *i.e.* an acceptor–donor–acceptor (A–D–A) architecture.

As shown in our previous studies,^{5,6} functionalization of the phosphorus centers results in a fine tuning of the band gaps by shifting the energy of the LUMO. In an attempt to illustrate

this effect, the reduction of the phosphorus centers of compounds **4a** and **4b** was investigated *via* the established protocols.^{6b} Upon treatment of the phosphole oxides with an excess of BH₃, both **4a** and **4b** exhibited a visibly increased emission intensity with unchanged emission color upon irradiation with a hand-held UV-lamp, very likely due to the formation of a phosphole–borane adduct, which has been previously reported for the inverse systems.^{6b}

Subsequently, an excess of triethylamine was added, which led to a visible blue shift of the emission for both investigated oligomers upon irradiation with UV-light. ³¹P NMR spectroscopy of the crude product mixture of the reduction of **4a** gave a single and very weak signal at $\delta^{31}\text{P}$ –20.3 ppm, indicating successful reduction to the phosphole. However, due to the extremely low solubility of the reduced oligomers in various solvents, purification attempts were unsuccessful and the reduced species could not be isolated.

Conclusions

In conclusion, we have succeeded in synthesizing and isolating a valuable monobrominated dithienophosphole building block, whose photophysical properties align nicely with those of the non- and dibrominated relatives. Subsequent cross-coupling reactions with a series of aryl linkers, exhibiting different architectures, provided some detailed insights into the modification of the photophysical properties of ‘dithienophosphole-rich’ conjugated materials. Our studies have indicated that proper choice of the linker components allows for selectively addressing the molar absorptivity, or the emission colors/quantum yields of the materials. Linkers that disrupt the conjugation were found to separate the oligomers into two independent chromophores with dramatically improved absorption coefficients of over 75 000 L mol^{–1} cm^{–1}, whereas linkers that promote conjugation over the whole scaffold provide for significantly red-shifted emission colors. Depending on the rigidity of the linker, remarkable photoluminescence quantum yields of up to 80% can be obtained for materials with an orange emission.

We are currently addressing the solubility issue of the extended oligomers by introducing additional solubilizing groups to the scaffold in order to investigate the fine tuning of the photophysical properties of the materials through phosphorus chemistry and to install improved processability features within these highly luminescent materials for a potential application in light-emitting devices.

Experimental section

General procedures

Reactions were carried out in dry glassware under inert gas atmosphere of purified nitrogen using Schlenk techniques. Solvents were dried using an MBraun solvent purification system. *N*-Bromosuccinimide (NBS), 1,3-phenyldiboronic acid, 1,4-phenyldiboronic acid, 4,4'-biphenyldiboronic acid, 9,9-dihexylfluorene-2,7-diboronic acid, caesium fluoride, sodium carbonate and tetrakis(triphenylphosphine)palladium(0) were purchased from Alfa Aesar, Sigma Aldrich or Strem and

used as received. 2,2'-Bithiophene-5,5'-diboronic acid bis(pinacol) ester¹¹ and dithieno(3,2-*b*:2',3'-*d*)phosphole oxide^{5b} were prepared according to literature methods. ¹H NMR, ¹³C NMR and ³¹P NMR spectra were recorded on a Bruker DMX-300 or Bruker Avance(-II, -III) 400 spectrometer. Chemical shifts are reported in ppm, referenced to external 85% H₃PO₄ (³¹P) or solvent signal (¹H, ¹³C). ¹³C and ³¹P NMR spectra were measured with proton decoupling. Elemental analysis was performed at the Department of Chemistry at the University of Calgary. It should be noted that some samples showed low carbon values even after column chromatography, indicating inherent problems with the measurement of these samples. Mass spectrometry was performed using a Finnigan SSQ700 or Bruker Daltonics AutoFlex III system. Optical spectroscopy was performed with dichloromethane solutions using a Jasco FP-6600 spectrometer and UV-Vis-NIR Cary 5000 spectrometer. Theoretical calculations have been carried out at the B3LYP/6-31G* level by using the GAUSSIAN 03 suite of programs.¹² This level of the theory has provided satisfactory results for phosphole–thiophene oligomers before.^{4–6,8} The geometries were fully optimized and at the resulting structures second derivatives were calculated.

X-Ray crystallography

Diffraction data were collected on a Nonius Kappa CCD diffractometer using monochromated MoK α radiation (λ = 0.71073 Å) at –100 °C. The data sets were corrected for Lorentz and polarization effects and empirical absorption correction was applied to the net intensities. The structure was solved by direct methods and refined using SHELX.¹³ After full-matrix least-square refinement of the nonhydrogen atoms with anisotropic thermal parameters, the hydrogen atoms were placed in calculated positions using a riding model.

Syntheses

2-Bromodithieno[3,2-*b*:2',3'-*d*]phosphole oxide 2. To a solution of dithieno[3,2-*b*:2',3'-*d*]phosphole oxide (2.57 g, 8.91 mmol) in 120 mL dimethylformamide (DMF), a solution of NBS (1.56 g, 8.91 mmol) in 25 mL DMF was dropwise (quickly) added at 0 °C. Immediately after addition, the mixture was poured on 500 mL of water. The yellow suspension was extracted with chloroform (3 × 100 mL). The combined organic phases were dried over magnesium sulfate and evaporated at reduced pressure to leave a yellow solid, which was purified by column chromatography on silica using chloroform/ethyl acetate (1/1) as eluent to give monobrominated product **2** (2.00 g, 61%) as yellow solid (found: C, 45.5; H, 2.1. C₁₄H₈OPS₂ requires C, 45.7; H, 2.2%); ¹H NMR (300 MHz; CDCl₃) 7.12 (1H, d, ³J_{H,P} = 2.5 Hz, 3-H), 7.16 (1H, dd, ³J_{H,P} = 2.3 Hz, ³J_{H,H} = 4.9 Hz, 5-H), 7.32 (1H, dd, ⁴J_{H,P} = 3.3 Hz, ³J_{H,H} = 4.9 Hz, 6-H), 7.39–7.49 (2H, m, *m*-Ph), 7.51–7.61 (1H, m, *p*-Ph), 7.67–7.77 (2H, m, *o*-Ph); ³¹P{¹H} NMR (121.5 MHz, CDCl₃) 18.9; ¹³C{¹H} NMR (100.6 MHz; CDCl₃) 114.8 (d, ³J_{C,P} = 18.1 Hz, Ar-Br), 126.1 (d, ³J_{C,P} = 14.9 Hz, Ar), 128.4 (d, ³J_{C,P} = 13.8 Hz, Ph), 128.9 (d, ³J_{C,P} = 15.1 Hz, Ar), 129.0 (d, ¹J_{C,P} = 101.8 Hz, *ipso*-Ph), 129.0 (d, ³J_{C,P} = 13.2 Hz, Ph), 130.8 (d, ³J_{C,P} = 11.5 Hz, Ar), 132.7 (d, ⁴J_{C,P} = 3.0 Hz, *p*-Ph), 137.7 (d, ¹J_{C,P} = 98.5 Hz, *ipso*-Ar), 138.8 (d, ¹J_{C,P} = 95.5 Hz,

ipso-Ar), 145.4 (d, $J_{C,P}$ = 24.6 Hz, Ar), 145.8 (d, $J_{C,P}$ = 22.2 Hz, Ar).

Compound 4a (1,4-benzene-bridged oligomer). 1,4-Phenyl-diboronic acid (83 mg, 0.5 mmol), [Pd(PPh₃)₄] (60 mg, 0.04 mmol) and BrS₂PO (400 mg, 1.1 mmol) were dissolved in 25 mL toluene and an aqueous solution of Na₂CO₃ (1 M, 10 mL) added. The emulsion was refluxed at 110 °C for 48 h. After cooling, the mixture was poured on 100 mL saturated NH₄Cl solution. The aqueous phase was extracted with chloroform (3 × 60 mL). The combined organic phases were dried over magnesium sulfate and evaporated at reduced pressure to leave an orange solid, which was purified by column chromatography on silica using chloroform/ethyl acetate (1/1) as eluent to give product **4a** (150 mg, 46%) as orange-yellow solid (found: C, 61.3; H, 3.4. C₃₄H₂₀O₂P₂S₄ requires C, 62.8; H, 3.1%); ¹H NMR (400 MHz; CD₂Cl₂) 7.18 (2H, dd, ³ $J_{H,P}$ = 2.4 Hz, ³ $J_{H,H}$ = 4.9 Hz, 5,5'-H, S₂PO), 7.38 (2H, dd, ⁴ $J_{H,P}$ = 3.3 Hz, ³ $J_{H,H}$ = 4.9 Hz, 6,6'-H, S₂PO), 7.41 (2H, d, ³ $J_{H,P}$ = 2.7 Hz, 3,3'-H, S₂PO), 7.42–7.48 (4H, m, *m*-Ph), 7.53–7.59 (2H, m, *p*-Ph), 7.61 (4H, s, Ph-bridge), 7.70–7.79 (4H, m, *o*-Ph); ³¹P{¹H} NMR (121.5 MHz, CDCl₃) 19.6; ¹³C{¹H} NMR (100.6 MHz; CD₂Cl₂) 122.2 (d, $J_{C,P}$ = 14.2 Hz, Ar), 126.4 (d, $J_{C,P}$ = 14.6 Hz, Ar), 126.7 (s, C-H, Ph-bridge), 129.5 (d, $J_{C,P}$ = 12.8 Hz, Ph), 129.6 (d, $J_{C,P}$ = 14.8 Hz, Ph), 129.8 (d, ¹ $J_{C,P}$ = 72.4 Hz, *ipso*-Ph), 131.4 (d, $J_{C,P}$ = 11.4 Hz, Ar), 133.0 (d, $J_{C,P}$ = 2.7 Hz, *p*-Ph), 133.8 (s, C-C, Ph-bridge), 139.2 (d, ¹ $J_{C,P}$ = 111.8 Hz, *ipso*-Ar), 141.0 (d, ¹ $J_{C,P}$ = 110.6 Hz, *ipso*-Ar), 145.0 (d, $J_{C,P}$ = 22.9 Hz, Ar), 146.4 (d, $J_{C,P}$ = 24.0 Hz, Ar), 148.0 (d, $J_{C,P}$ = 14.1 Hz, Ar); HRMS: m/z 649.9850 (M⁺. C₃₄H₂₀O₂P₂S₄ requires 649.9821).

Compound 4b (1,3-benzene-bridged oligomer). 1,3-Phenyl-diboronic acid (80 mg, 0.5 mmol), [Pd(PPh₃)₄] (58 mg, 0.04 mmol) and BrS₂PO (370 mg, 1.0 mmol) were dissolved in 20 mL toluene and an aqueous solution of Na₂CO₃ (1 M, 10 mL) added. The emulsion was refluxed at 110 °C for 48 h. After cooling, the mixture was poured on 100 mL saturated NH₄Cl solution. The aqueous phase was extracted with chloroform (3 × 50 mL). The combined organic phases were dried over magnesium sulfate and evaporated at reduced pressure to leave an orange solid, which was purified by column chromatography on silica using chloroform/ethyl acetate (1/1) as eluent to give product **4b** (132 mg, 42%) as yellow solid (found: C, 61.2; H, 3.3. C₃₄H₂₀O₂P₂S₄ requires C, 62.8; H, 3.1%); ¹H NMR (400 MHz; CDCl₃) 7.16 (2H, dd, ³ $J_{H,P}$ = 2.4 Hz, ³ $J_{H,H}$ = 4.9 Hz, 5,5'-H, S₂PO), 7.31 (2H, dd, ⁴ $J_{H,P}$ = 3.3 Hz, ³ $J_{H,H}$ = 4.9 Hz, 6,6'-H, S₂PO), 7.37 (2H, d, ³ $J_{H,P}$ = 2.5 Hz, 3,3'-H, S₂PO), 7.38–7.49 (7H, complex area, *m*-Ph and Ph-bridge), 7.50–7.59 (2H, m, *p*-Ph), 7.66 (1H, t, ⁴ $J_{H,H}$ = 1.5 Hz, Ph-bridge), 7.77 (4H, br dd, ³ $J_{H,H}$ = 7.9 Hz, ³ $J_{H,P}$ = 13.3 Hz, *o*-Ph); ³¹P{¹H} NMR (121.5 MHz, CDCl₃) 19.6; ¹³C{¹H} NMR (100.6 MHz; CDCl₃) 122.0 (d, $J_{C,P}$ = 14.2 Hz, Ar), 122.8 (s, Ph-bridge), 122.9 (s, Ph-bridge), 125.5 (s, Ph-bridge), 126.1 (d, $J_{C,P}$ = 14.6 Hz, Ar), 128.8 (d, $J_{C,P}$ = 15.1 Hz, Ph), 129.0 (d, $J_{C,P}$ = 13.2 Hz, Ph), 129.4 (d, ¹ $J_{C,P}$ = 106.0 Hz, *ipso*-Ph), 130.8 (d, $J_{C,P}$ = 11.4 Hz, Ar), 132.5 (d, $J_{C,P}$ = 2.8 Hz, *p*-Ph), 134.2 (s, C-C, Ph-bridge), 138.3 (d, ¹ $J_{C,P}$ = 112.5 Hz, *ipso*-Ar), 140.0 (d, ¹ $J_{C,P}$ = 111.3 Hz, *ipso*-Ar), 144.6

(d, $J_{C,P}$ = 23.1 Hz, Ar), 145.9 (d, $J_{C,P}$ = 24.5 Hz, Ar), 147.2 (d, $J_{C,P}$ = 14.4 Hz, Ar). It should be noted that the high-field peak of the signal at 129.4 ppm overlaps with the signal at 129.0 ppm, resulting in a shoulder rather than a distinct peak. HRMS: m/z 649.9821 (M⁺. C₃₄H₂₀O₂P₂S₄ requires 649.9821).

Compound 4c (4,4'-biphenyl-bridged oligomer). 4,4'-Biphenyl-diboronic acid (150 mg, 0.6 mmol), [Pd(PPh₃)₄] (75 mg, 0.07 mmol) and BrS₂PO (478 mg, 1.3 mmol) were dissolved in 35 mL toluene and an aqueous solution of Na₂CO₃ (1 M, 15 mL) added. The emulsion was refluxed at 110 °C for 72 h. After cooling, the mixture was poured on 150 mL water. The aqueous phase was extracted with chloroform (5 × 60 mL). The combined organic phases were dried over magnesium sulfate and evaporated at reduced pressure to leave an orange-brown solid, which was washed repeatedly with hot hexanes and acetone to give product **4c** (185 mg, 41%) as light orange solid. ¹H NMR (300 MHz; CDCl₃) 7.18 (2H, dd, ⁴ $J_{H,P}$ = 2.4 Hz, ³ $J_{H,H}$ = 4.9 Hz, 5,5'-H, S₂PO), 7.32 (2H, dd, ³ $J_{H,P}$ = 3.3 Hz, ³ $J_{H,H}$ = 4.9 Hz, 6,6'-H, S₂PO), 7.39 (2H, d, ³ $J_{H,P}$ = 2.7 Hz, 3,3'-H, S₂PO), 7.42–7.50 (4H, m, *m*-Ph), 7.52–7.59 (2H, m, *p*-Ph), 7.63 (8H, br s, Ph₂-bridge), 7.79 (4H, br dd, ³ $J_{H,H}$ = 7.0 Hz, ³ $J_{H,P}$ = 13.5 Hz, *o*-Ph); ³¹P{¹H} NMR (121.5 MHz, CDCl₃) 19.2; ¹³C{¹H} NMR (100.6 MHz; DMSO-d₆) 122.4 (d, $J_{C,P}$ = 14.4 Hz, Ar), 125.8 (s, C-H, biphenyl), 126.1 (d, $J_{C,P}$ = 14.5 Hz, Ar), 127.1 (s, C-H, biphenyl), 129.1 (d, $J_{C,P}$ = 12.7 Hz, Ph), 130.2 (d, ¹ $J_{C,P}$ = 106.9 Hz, *ipso*-Ph), 130.5 (d, $J_{C,P}$ = 11.3 Hz, Ar), 130.8 (d, $J_{C,P}$ = 14.7 Hz, Ph), 132.1 (s, C-C, biphenyl), 132.6 (d, $J_{C,P}$ = 2.7 Hz, *p*-Ph), 138.2 (d, ¹ $J_{C,P}$ = 109.2 Hz, *ipso*-Ar), 138.6 (s, C-C, biphenyl), 139.9 (d, ¹ $J_{C,P}$ = 109.2 Hz, *ipso*-Ar), 143.2 (d, $J_{C,P}$ = 23.0 Hz, Ar), 144.7 (d, $J_{C,P}$ = 24.0 Hz, Ar), 147.0 (d, $J_{C,P}$ = 14.2 Hz, Ar).

Compound 4d (9,9-dihexylfluorene-bridged oligomer). 9,9-Dihexylfluorene-2,7-diboronic acid (296 mg, 0.7 mmol), [Pd(PPh₃)₄] (85 mg, 0.07 mmol) and BrS₂PO (540 mg, 1.5 mmol) were dissolved in 30 mL toluene and an aqueous solution of Na₂CO₃ (1 M, 15 mL) added. The emulsion was refluxed at 110 °C for 48 h. After cooling, the mixture was poured on 100 mL water. The aqueous phase was extracted with chloroform (3 × 60 mL). The combined organic phases were dried over magnesium sulfate and evaporated at reduced pressure to leave an orange solid, which was washed repeatedly with hexanes and diethyl ether to give product **4d** (318 mg, 50%) as orange solid (found: C, 69.1; H, 5.1. C₅₃H₄₈O₂P₂S₄ requires C, 70.2; H, 5.3%); ¹H NMR (400 MHz; CDCl₃) 0.75 (6H, t, ³ $J_{H,H}$ = 7.0 Hz, CH₃), 0.96–1.34 (16H, m, CH₂), 1.99 (4H, t, ³ $J_{H,H}$ = 8.0 Hz, α-CH₂), 7.19 (2H, dd, ⁴ $J_{H,P}$ = 2.4 Hz, ³ $J_{H,H}$ = 4.9 Hz, 5,5'-H, S₂PO), 7.32 (2H, dd, ³ $J_{H,P}$ = 3.3 Hz, ³ $J_{H,H}$ = 4.9 Hz, 6,6'-H, S₂PO), 7.42 (2H, d, ³ $J_{H,P}$ = 2.7 Hz, 3,3'-H, S₂PO), 7.44–7.52 (6H, m, *m*-Ph and 1,8-H, fluorene), 7.52–7.60 (4H, m, *p*-Ph and 3,6-H, fluorene), 7.69 (2H, br d, 4,5-H, fluorene), 7.82 (4H, br dd, ³ $J_{H,H}$ = 7.0 Hz, ³ $J_{H,P}$ = 13.5 Hz, *o*-Ph); ³¹P{¹H} NMR (121.5 MHz, CDCl₃) 19.6; ¹³C{¹H} NMR (100.6 MHz; CDCl₃) 14.0 (s, CH₃), 22.5 (s, CH₂), 23.7 (s, CH₂), 29.6 (s, CH₂), 31.4 (s, CH₂), 40.3 (s, α-CH₂), 55.4 (s, 9-C, fluorene), 119.9 (s, C-H, fluorene), 120.5 (s, C-H, fluorene), 121.3 (d, $J_{C,P}$ = 14.2 Hz, Ar), 124.9 (s, C-H, fluorene), 126.1 (d, $J_{C,P}$ = 14.7 Hz, Ar),

128.4 (d, $J_{C,P}$ = 15.1 Hz, Ph), 129.0 (d, $J_{C,P}$ = 13.0 Hz, Ph), 129.7 (d, $^1J_{C,P}$ = 108.0 Hz, *ipso*-Ph), 130.9 (d, $J_{C,P}$ = 11.3 Hz, Ar), 132.5 (s, C-C, fluorene), 132.5 (d, $J_{C,P}$ = 2.7 Hz, *p*-Ph), 138.2 (d, $^1J_{C,P}$ = 112.4 Hz, *ipso*-Ar), 140.1 (d, $^1J_{C,P}$ = 111.6 Hz, *ipso*-Ar), 140.7 (s, C-C, fluorene), 143.8 (d, $J_{C,P}$ = 23.0 Hz, Ar), 146.2 (d, $J_{C,P}$ = 24.2 Hz, Ar), 149.1 (d, $J_{C,P}$ = 14.4 Hz, Ar), 152.0 (s, C-C, fluorene); HR-MALDI/TOF-MS: m/z 929.1938 (M^+ + Na. $C_{53}H_{48}NaO_2P_2S_4$ requires 929.1964).

Compound 5 (5,5'-bithiophene-bridged oligomer). 2,2'-Bithiophene-5,5'-diboronic acid bis(pinacol) ester (321 mg, 0.8 mmol), $[Pd(PPh_3)_4]$ (90 mg, 0.06 mmol), caesium fluoride (770 mg, 5.1 mmol) and BrS_2PO (620 mg, 1.7 mmol) were dissolved in 50 mL tetrahydrofuran and refluxed at 70 °C for 72 h. After cooling, the mixture was reduced to dryness and the residue taken up in 150 mL chloroform. The solution was extracted with saturated NH_4Cl solution and water. The organic phase was dried over magnesium sulfate and evaporated at reduced pressure to leave an orange solid, which was repeatedly washed with cold diethyl ether to give product **5** (330 mg, 58%) as orange-red solid (found: C, 57.9; H, 3.1. $C_{36}H_{20}O_2P_2S_6$ requires C, 58.5; H, 2.7%); 1H NMR (300 MHz; $CDCl_3$) 7.08 (4H, br s, bridge), 7.17 (2H, dd, $^3J_{H,P}$ = 2.4 Hz, $^3J_{H,H}$ = 4.9 Hz, 5,5'-H, S_2PO), 7.19 (2H, d, $^3J_{H,P}$ = 2.7 Hz, 3,3'-H, S_2PO), 7.31 (2H, dd, $^4J_{H,P}$ = 3.4 Hz, $^3J_{H,H}$ = 4.9 Hz, 6,6'-H, S_2PO), 7.41–7.50 (4H, m, *m*-Ph), 7.52–7.60 (2H, m, *p*-Ph), 7.77 (4H, br dd, $^3J_{H,H}$ = 7.0 Hz, $^3J_{H,P}$ = 13.5 Hz, *o*-Ph); $^{31}P\{^1H\}$ NMR (121.5 MHz, $CDCl_3$) 19.4; $^{13}C\{^1H\}$ NMR (100.6 MHz; $CDCl_3$) 121.9 (d, $J_{C,P}$ = 14.4 Hz, Ar), 124.8 (s, C-H, bridge), 125.1 (s, C-H, bridge), 126.2 (d, $J_{C,P}$ = 14.6 Hz, Ar), 128.7 (d, $J_{C,P}$ = 14.7 Hz, Ph), 129.0 (d, $J_{C,P}$ = 13.1 Hz, Ph), 129.4 (d, $^1J_{C,P}$ = 103.1 Hz, *ipso*-Ph), 130.9 (d, $J_{C,P}$ = 11.4 Hz, Ar), 132.6 (d, $J_{C,P}$ = 2.8 Hz, *p*-Ph), 135.2 (s, C-C, bridge), 136.4 (s, C-C, bridge), 138.4 (d, $^1J_{C,P}$ = 112.6 Hz, *ipso*-Ar), 140.0 (d, $^1J_{C,P}$ = 110.9 Hz, *ipso*-Ar), 140.6 (d, $J_{C,P}$ = 15.4 Hz, Ar), 143.7 (d, $J_{C,P}$ = 22.8 Hz, Ar), 145.8 (d, $J_{C,P}$ = 24.3 Hz, Ar); HR-MALDI/TOF-MS: m/z 760.9165 (M^+ + Na. $C_{36}H_{20}NaO_2P_2S_6$ requires 760.9155).

Acknowledgements

Financial support by Natural Sciences and Engineering Research Council (NSERC) of Canada and by the Canada Foundation for Innovation (CFI) is gratefully acknowledged. We thank Alberta Ingenuity for a student scholarship (S.D.) and for a New Faculty Award (T.B.). The authors thank Prof. Todd Sutherland (University of Calgary) for helpful discussions and Prof. Dr Jun Okuda (RWTH Aachen University) for his support.

Notes and references

- (a) *Handbook of Conducting Polymers*, ed. T. A. Skotheim and J. R. Reynolds, CRC Press, Boca Raton, FL, 3rd edn, 2006; (b) *Organic Light Emitting Devices*, ed. K. Müllen and U. Scherf, Wiley-VCH, Weinheim, 2005; (c) *Handbook of Oligo- and Polythiophenes*, ed. D. Fichou, Wiley-VCH, Weinheim, 1998.
- (a) M. J. D. Bosdet and W. E. Piers, *Can. J. Chem.*, 2009, **87**, 8; (b) M. Elbing and G. C. Bazan, *Angew. Chem., Int. Ed.*, 2008, **47**, 834; (c) S. Yamaguchi and A. Wakamiya, *Pure Appl. Chem.*, 2006, **78**, 1413; (d) F. Jäkle, *Coord. Chem. Rev.*, 2006, **250**, 1107; (e) C. D. Entwistle and T. B. Marder, *Chem. Mater.*, 2004, **16**, 4574.
- (a) A. C. Grimsdale, K. L. Chan, R. E. Martin, P. G. Jokisz and A. B. Holmes, *Chem. Rev.*, 2009, **109**, 897; (b) M. Shimizu, H. Tatsumi, K. Mochida, K. Oda and T. Hiyama, *Chem.-Asian J.*, 2008, **3**, 1238; (c) S. Yamaguchi, C. Xu and T. Okamoto, *Pure Appl. Chem.*, 2006, **78**, 721; (d) S. Yamaguchi and K. Tamao, *Chem. Lett.*, 2005, **34**, 2; (e) M. Hissler, P. W. Dyer and R. Réau, *Coord. Chem. Rev.*, 2003, **244**, 1.
- (a) T. Baumgartner and R. Réau, *Chem. Rev.*, 2006, **106**, 4681 (*Chem. Rev.*, 2007, **107**, 303) Correction; (b) M. G. Hobbs and T. Baumgartner, *Eur. J. Inorg. Chem.*, 2007, 3611; (c) Y. Matano and H. Imahori, *Org. Biomol. Chem.*, 2009, **7**, 1258; (d) J. Crassous and R. Réau, *Dalton Trans.*, 2008, 6865; (e) A. Fukazawa, Y. Ichihashi, Y. Kosaka and S. Yamaguchi, *Chem.-Asian J.*, 2009, **4**, 1729; (f) A. Saito, T. Miyajima, M. Nakashima, T. Fukushima, H. Kaji, Y. Matano and H. Imahori, *Chem.-Eur. J.*, 2009, **15**, 10000; (g) T. Agou, Md. D. Hossain, T. Kawashima, K. Kamada and K. Ohta, *Chem. Commun.*, 2009, 6762.
- (a) T. Baumgartner, T. Neumann and B. Wirges, *Angew. Chem.*, 2004, **116**, 6323 (*Angew. Chem., Int. Ed.*, 2004, **43**, 6197); (b) T. Baumgartner, W. Bergmans, T. Kárpáti, T. Neumann, M. Nieger and L. Nyulási, *Chem.-Eur. J.*, 2005, **11**, 4687.
- (a) T. Neumann, Y. Dienes and T. Baumgartner, *Org. Lett.*, 2006, **8**, 495; (b) Y. Dienes, S. Durben, T. Kárpáti, T. Neumann, U. Englert, L. Nyulási and T. Baumgartner, *Chem.-Eur. J.*, 2007, **13**, 7487; (c) Y. Dienes, M. Eggenstein, T. Kárpáti, T. C. Sutherland, L. Nyulási and T. Baumgartner, *Chem.-Eur. J.*, 2008, **14**, 9878; (d) Y. Ren, Y. Dienes, S. Hettel, M. Parvez, B. Hoge and T. Baumgartner, *Organometallics*, 2009, **28**, 734; (e) C. Romero-Nieto, S. Merino, J. Rodríguez-López and T. Baumgartner, *Chem.-Eur. J.*, 2009, **15**, 4135.
- (a) S. Durben, Y. Dienes and T. Baumgartner, *Org. Lett.*, 2006, **8**, 5893; (b) S. Durben, D. Nickel, R. A. Krueger and T. Baumgartner, *J. Polym. Sci., Part A: Polym. Chem.*, 2008, **46**, 8179; (c) C. Romero-Nieto, S. Durben, I. M. Kormos and T. Baumgartner, *Adv. Funct. Mater.*, 2009, **19**, 3625.
- D. R. Bai, C. Romero-Nieto and T. Baumgartner, *Dalton Trans.*, 2010, **39**, 1250.
- Y. Dienes, U. Englert and T. Baumgartner, *Z. Anorg. Allg. Chem.*, 2009, **635**, 238.
- Metal-Catalyzed Cross-Coupling Reactions*, ed. A. de Meijere and F. Diederich, Wiley-VCH, Weinheim, 2nd edn, 2004.
- H. Usta, G. Lu, A. Facchetti and T. J. Marks, *J. Am. Chem. Soc.*, 2006, **128**, 9034.
- M. J. Frisch, G. W. Trucks, H. B. Schlegel, G. E. Scuseria, M. A. Robb, J. R. Cheeseman, J. A. Jr. Montgomery, T. Vreven, K. N. Kudin, J. C. Burant, J. M. Millam, S. S. Iyengar, J. Tomasi, V. Barone, B. Mennucci, M. Cossi, G. Scalmani, N. Rega, G. A. Petersson, H. Nakatsuji, M. Hada, M. Ehara, K. Toyota, R. Fukuda, J. Hasegawa, M. Ishida, T. Nakajima, Y. Honda, O. Kitao, H. Nakai, M. Klene, X. Li, J. E. Knox, H. P. Hratchian, J. B. Cross, V. Bakken, C. Adamo, J. Jaramillo, R. Gomperts, R. E. Stratmann, O. Yazyev, A. J. Austin, R. Cammi, C. Pomelli, J. W. Ochterski, P. Y. Ayala, K. Morokuma, G. A. Voth, P. Salvador, J. J. Dannenberg, V. G. Zakrzewski, S. Dapprich, A. D. Daniels, M. C. Strain, O. Farkas, D. K. Malick, A. D. Rabuck, K. Raghavachari, J. B. Foresman, J. V. Ortiz, Q. Cui, A. G. Baboul, S. Clifford, J. Cioslowski, B. B. Stefanov, G. Liu, A. Liashenko, P. Piskorz, I. Komaromi, R. L. Martin, D. J. Fox, T. Keith, M. A. Al-Laham, C. Y. Peng, A. Nanayakkara, M. Challacombe, P. M. W. Gill, B. Johnson, W. Chen, M. W. Wong, C. Gonzalez and J. A. Pople, *GAUSSIAN 03, Revision E.01*, Gaussian Inc., Wallingford, CT, 2007.
- G. M. Sheldrick, *Acta Crystallogr., Sect. A: Found. Crystallogr.*, 2008, **64**, 112.